ENGINEERING TRANSACTIONS • *Engng. Trans.* • **44**, 2, 207–228, 1996
Polish Academy of Sciences • Institute of Fundamental Technological Research

THREE-DIMENSIONAL SLIP-LINE FIELD THEORY WITH ROTATIONAL CONTINUITY

R. L. BISH (MELBOURNE)

For cold-worked metal bodies undergoing plastic deformation along well-defined loading paths, a three-dimensional slip-line field theory is developed, taking into account the new principle of rotation-rate continuity. It is shown that the slip-line network is always confined to one of the three families of principal stress surfaces and that the strain rate normal to those surfaces vanishes. Further, the ratio of the radii of curvature of the slip-lines in the plane tangent to the net remains constant. This condition, in turn, imposes restrictions on the geometric configurations that are allowed for the net boundary. The velocity hodograph always has one of these configurations.

1. INTRODUCTION

Any region within a plastically deforming metal body, if that region is small enough, will exhibit mechanical anisotropy and, conseqeuntly, will rotate so as to keep its crystallographic planes of slip aligned with the principal shear surfaces. From this hypothesis, a fundamental principle emerges to complete and extend the classical slip-line field theory, and this principle, very simply, states that the (vector) rate of rotation within the deforming body must remain (spatially) continuous. Otherwise, any two adjacent deforming elements of the body could not maintain their slip-planes parallel to the local surfaces of principal shear stress which, by equilibrium, are required to remain smooth. This new principle of plasticity serves to resolve a long standing question, and represents one of the principal reasons for the present paper.

PRANDTL [2], in 1920, in publishing the first solution to a slip-line field problem, that of the plane-strain compression of a metal mass, utilized cycloidal slip-lines. Some three decades later HILL [3] published a second and (geometrically) very different solution to this problem. Books [4, 5] concerning the subject of plasticity and published before or during the 1950's, continued to present Prandtl's solution to the plane-strain compression problem. On the other hand, most of the books [6] published after that period present

only Hill's solution to the plane-strain compression problem. We shall learn that Hill's solution, unlike that of Prandtl, complies with the new principle of continuity of the rotation rate although, of course, Hill could not had known this principle when he published his equiangular slip-line net.

There are many problems of plastic deformation of industrial significance, that are three-dimensional while, most luckily, with the inclusion of the new hypothesis, a three-dimensional slip-line field theory forms a natural development. The theory to be presented here is, for these reasons, quite general.

2. Yield conditions and the flow rule

Tresca's yield criterion will govern the process of yielding in a cold-worked metal body in which the crystal-grains are aligned with their crystallographic slip-planes parallel to the surfaces of principal shear. The yield surface, in σ_{ij}-space, will therefore be a hexagonal cylinder having plane faces described by

$$
\begin{aligned}
&\sigma_2 - \sigma_1 = 2k, && \sigma_2 > \sigma_3 > \sigma_1,\\
&\sigma_1 - \sigma_2 = 2k, && \sigma_1 > \sigma_3 > \sigma_2,\\
&\sigma_3 - \sigma_2 = 2k, && \sigma_3 > \sigma_1 > \sigma_2,\\
&\sigma_2 - \sigma_3 = 2k, && \sigma_2 > \sigma_1 > \sigma_3,\\
&\sigma_1 - \sigma_3 = 2k, && \sigma_1 > \sigma_2 > \sigma_3,\\
&\sigma_3 - \sigma_1 = 2k, && \sigma_3 > \sigma_2 > \sigma_1,
\end{aligned}
\tag{2.1}
$$

where k is the shear yield stress of the solid.

On the other hand, by Prager's flow rule [7], if

$$h(\sigma_1, \sigma_2, \sigma_3) = 0$$

denotes the yield surface in σ_{ij}-space, then

$$d\varepsilon_{ij} = \frac{\partial h}{\partial \sigma_{ij}} d\lambda, \tag{2.2}$$

where λ is a multiplier. From (2.1) it therefore follows that

$$d\varepsilon_3 = 0 \quad \text{for} \quad \sigma_1 - \sigma_2 = \pm 2k, \tag{2.3}$$

$$d\varepsilon_1 = 0 \quad \text{for} \quad \sigma_2 - \sigma_3 = \pm 2k, \tag{2.4}$$

$$d\varepsilon_2 = 0 \quad \text{for} \quad \sigma_3 - \sigma_1 = \pm 2k. \tag{2.5}$$

Thus deformation is such that the Hencky-Prandl net lies in a principal surface in the solid, while the strain-rate normal to that surface vanishes. Cases where the stress-point lies on an edge of the yield surface are included in the analysis [8]. We may write, in place of (2.3)-(2.5),

$$\dot{\varepsilon}_{nn} = 0, \tag{2.6}$$

where n is the coordinate normal to the principal surface in the deforming body, on which the net lies.

It is clear that the von Mises yield condition must also be applicable to a system such as that under consideration, since this criterion stipulates that yield commences when the shear elastic energy per unit volume within the deforming body reaches a critical level. Thus if

$$J_2 = \frac{1}{2}\tau_{ij}\tau_{ij},$$

where τ_{ij} is the stress deviation tensor, (2.2) leads [9] to

$$d\varepsilon_{ij} = \frac{\partial h}{\partial J_2}\tau_{ij}d\lambda,$$

whence, by (2.6),

$$\tau_{nn} = 0,$$

or

$$\sigma_{nn} = \sigma, \tag{2.7}$$

where σ equals one half of the sum of the two principal stresses acting in the plane tangent to the principal surface, of normal n, within the deforming body. Moreover, substituting this result back into the von Mises yield condition, we recover Tresca's yield condition.

3. Stress-equilibrium

Let the n-surfaces contain principal shear lines along which α and β denote the coordinates. Moreover, let h_n, h_α and h_β denote the scale factors for the (n, α, β) system of coordinates. Then, according to (2.6) or to the results established in an earlier article [10], the distance between any two n-surfaces must remain constant. Since $h_n\,dn$ equals the distance between

two n-surfaces, corresponding to n-values of n and $h_n\,dn$, it follows that the conditions for this constancy or spacing are:

$$\frac{\partial h_n}{\partial \alpha} = 0, \tag{3.1}$$

$$\frac{\partial h_n}{\partial \beta} = 0. \tag{3.2}$$

We also note that

$$\sigma_{n\alpha} = \sigma_{n\beta} = 0,$$

while we write

$$\sigma_{\alpha\beta} = \tau, \qquad \sigma_{\alpha\alpha} = \sigma_{\beta\beta} = \sigma.$$

The stress-equilibrium equation (A.3) then becomes

$$\frac{\partial \sigma_{nn}}{\partial n} + \frac{(\sigma_{nn} - \sigma)}{h_\alpha}\frac{\partial h_\alpha}{\partial n} + \frac{(\sigma_{nn} - \sigma)}{h_\beta}\frac{\partial h_\beta}{\partial n} = 0,$$

while by (B.11), (B.12) and (2.7), Eqs. (A.1) and (A.2) and this equation lead to

$$\frac{\partial \sigma}{h_\alpha \partial \alpha} - 2\tau\frac{\partial \phi}{h_\alpha \partial \alpha} + \frac{\partial \tau}{h_\beta \partial \beta} = 0, \tag{3.3}$$

$$\frac{\partial \sigma}{h_\beta \partial \beta} + 2\tau\frac{\partial \phi}{h_\beta \partial \beta} + \frac{\partial \tau}{h_\alpha \partial \alpha} = 0, \tag{3.4}$$

$$\frac{\partial \sigma}{\partial n} = 0, \tag{3.5}$$

where ϕ is the net angle, measured anti-clockwise about the n-axis (Fig. 1).

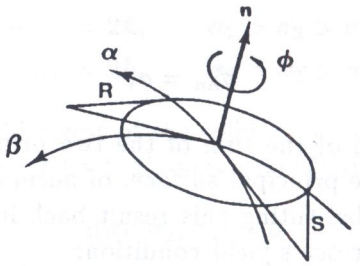

FIG. 1. Principal stress surface containing the α- and β-slip-lines. The net angle, ϕ, is measured in the anti-clockwise sense.

In the case of an ideal solid, the yield condition takes the form $\tau = k$, where k is the shear yield-stress of the solid, and substituting this condition into (3.3) and (3.4) leads to

$$\frac{\partial^2 \phi}{\partial \alpha \partial \beta} = 0. \tag{3.6}$$

On the other hand, the new principle of continuity of the rotation rate provides an independent second equation governing ϕ to be considered below.

4. Harmonic character of ϕ

If $\boldsymbol{\omega}$ denotes the rotation-rate vector, it may be shown [10] that

$$\operatorname{curl}\boldsymbol{\omega} = 0, \tag{4.1}$$

and using the formulae (in which v denotes the velocity vector of a continuous velocity field that replaces the actual velocities):

$$\dot{\varepsilon} = \frac{1}{2}\left\{\operatorname{grad}\mathbf{v} + (\operatorname{grad}\mathbf{v})^T\right\},$$

$$\operatorname{div}\mathbf{v} = 0,$$

$$\boldsymbol{\omega} = (1/2)\operatorname{curl}\mathbf{v},$$

Eq.(4.1) leads to

$$\operatorname{div}\dot{\boldsymbol{\epsilon}} = 0. \tag{4.2}$$

Using the conditions

$$\dot{\varepsilon}_{n\alpha} = \dot{\varepsilon}_{n\beta} = 0,$$

and writing

$$\dot{\varepsilon}_{\alpha\alpha} = \dot{\varepsilon}_{\beta\beta} = \dot{e},$$
$$\dot{\varepsilon}_{\alpha\beta} = \dot{\gamma},$$

Eq. (4.2) reduces, by (3.1) and (3.2), by analogy with th equations of Appendix A, to

$$\frac{\partial \dot{e}}{h_\alpha \partial\alpha} + \frac{2\dot{\gamma}}{h_\alpha h_\beta}\frac{\partial h_\alpha}{\partial\beta} + \frac{\partial\dot{\gamma}}{h_\beta\partial\beta} = 0, \tag{4.3}$$

$$\frac{\partial \dot{e}}{h_\beta \partial\beta} + \frac{2\dot{\gamma}}{h_\alpha h_\beta}\frac{\partial h_\beta}{\partial\alpha} + \frac{\partial\dot{\gamma}}{h_\alpha\partial\alpha} = 0, \tag{4.4}$$

$$\frac{\partial\dot{\varepsilon}_{nn}}{\partial n} + \frac{(\dot{\varepsilon}_{nn} - \dot{e})}{h_\alpha}\frac{\partial h_\alpha}{\partial n} + \frac{(\dot{\varepsilon}_{nn} - \dot{e})}{h_\beta}\frac{\partial h_\beta}{\partial n} = 0. \tag{4.5}$$

On the other hand,

$$2\dot{e} + \dot{\varepsilon}_{nn} = 0,$$

so that, by (2.6)

$$\dot{e} = 0, \tag{4.6}$$

and (4.5) is satisfied, while from (4.3) and (4.4) we obtain

$$\frac{\partial}{\partial\alpha}\left(\frac{1}{h_\alpha}\frac{\partial h_\alpha}{\partial\beta}\right) = \frac{\partial}{\partial\beta}\left(\frac{1}{h_\beta}\frac{\partial h_\beta}{\partial\alpha}\right),$$

or, on subsituting from (B.11) and (B.12),

$$\frac{\partial}{\partial\alpha}\left(\frac{h_\beta}{h_\alpha}\frac{\partial\phi}{\partial\alpha}\right) + \frac{\partial}{\partial\beta}\left(\frac{h_\alpha}{h_\beta}\frac{\partial\phi}{\partial\beta}\right) = 0. \tag{4.7}$$

Because, moreover, n is measured along the principal axis and ϕ denotes an (actual) physical rotation it follows, since there can be no torsion along the n-axis, that

$$\frac{\partial\phi}{\partial n} = 0. \tag{4.8}$$

From Eqs. (3.1), (3.2), (4.7) and (4.8) it follows, from the three-dimensional expression, (B.15) that

$$\nabla^2\phi = 0. \tag{4.9}$$

5. Consistency

Let us now let R and S be equal, respectively, to the radii of curvature of the curves that are formed by intersections of the slip-surfaces with the local plane tangent to the n-surface (Fig. 2). Then, if we subsitute for the derivatives of h_α and h_β in (4.9) (in view of (3.1), (3.2), (4.6) and (4.7)), the results (B.11) and (B.12), and, if we substitute the scale factors from (B.13) and (B.14), we obtain

$$\frac{\partial}{\partial\alpha}\left(\frac{S}{R}\frac{\partial\phi}{\partial\beta}\right) + \frac{\partial}{\partial\beta}\left(\frac{R}{S}\frac{\partial\phi}{\partial\alpha}\right) = 0. \tag{5.1}$$

If we now write

$$\frac{S}{R} = C, \tag{5.2}$$

C denoting a constant, then (5.1) becomes

$$\left(C + \frac{1}{C}\right)\frac{\partial^2\phi}{\partial\alpha\partial\beta} = 0,$$

which is the same as (3.6) because C is required to remain real. Therefore (5.2) is the condition that ensures the consistency between (4.9) and (3.6). We are led, therefore, to the study of Eq. (5.2).

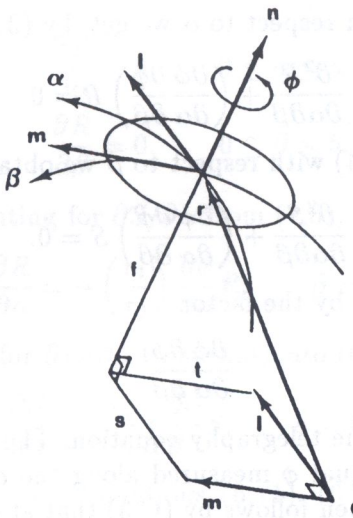

FIG. 2. Three-dimensional extension of Mikhlin's coordinate system.

6. RADII OF CURVATURE

Differentiating (B.13) with respect to β we obtain, by (3.6) and (B.11),

$$\left(\frac{\partial R}{\partial \beta} + h_\beta\right)\frac{\partial \phi}{\partial \alpha} = 0,$$

while, differentiating (B.14) with respect to α leads, by (3.6) and (B.12), to

$$\left(\frac{\partial S}{\partial \alpha} + h_\alpha\right)\frac{\partial \phi}{\partial \beta} = 0.$$

If R and S remain finite, these equations demand that

$$\frac{\partial R}{\partial \beta} + h_\beta = 0, \tag{6.1}$$

$$\frac{\partial S}{\partial \alpha} + h_\alpha = 0, \tag{6.2}$$

and substituting for h_β in (6.1), the result (B.14), we obtain

$$\frac{\partial R}{\partial \beta} = \left(\frac{\partial \phi}{\partial \beta}\right) S, \tag{6.3}$$

while from (6.2), on substituting from (B.13), we also obtain

$$\frac{\partial S}{\partial \alpha} = -\left(\frac{\partial \phi}{\partial \alpha}\right) R. \tag{6.4}$$

Differentiating (6.3) with respect to α we get, by (3.6) and (6.4),

$$\frac{\partial^2 R}{\partial\alpha\partial\beta} + \left(\frac{\partial\phi}{\partial\alpha}\frac{\partial\phi}{\partial\beta}\right) R = 0 \tag{6.5}$$

while, differentiating (6.4) with respect to β we obtain, by (3.6) and (6.3),

$$\frac{\partial^2 S}{\partial\alpha\partial\beta} + \left(\frac{\partial\phi}{\partial\alpha}\frac{\partial\phi}{\partial\beta}\right) S = 0. \tag{6.6}$$

Dividing these equations by the factor

$$\frac{\partial\phi}{\partial\alpha}\frac{\partial\phi}{\partial\beta}$$

we obtain, using (3.6), the telegraphy equation. The two independent variables in this equation equal ϕ measured along the α- and β-lines. Setting $\phi(0,0)$ equal to zero it then follows by (C.3) that at $(\alpha,\beta) = (a,b)$

$$\begin{aligned} R = r_1 J_0\Big\{2\sqrt{(\phi(a,0)\phi(0,b)}\Big\} \\ + \int_{\substack{0\\ \beta=0}}^{a} J_0\Big\{2\sqrt{(\phi(a,0)-\phi(\alpha,0))\phi(0,b)}\Big\}\frac{\partial R}{\partial\alpha}d\alpha \\ + \int_{\substack{0\\ \alpha=0}}^{b} J_0\Big\{2\sqrt{\phi(a,0)(\phi(0,b)-\phi(0,\beta))}\Big\}\frac{\partial R}{\partial\beta}d\beta, \end{aligned}$$

and

$$\begin{aligned} S = r_2 J_0\Big\{2\sqrt{\phi(a,0)\phi(0,b)}\Big\} \\ + \int_{\substack{0\\ \beta=0}}^{a} J_0\Big\{2\sqrt{(\phi(a,0)-\phi(\alpha,0))\phi(0,b)}\Big\}\frac{\partial S}{\partial\alpha}d\alpha \\ + \int_{\substack{0\\ \alpha=0}}^{b} J_0\Big\{2\sqrt{\phi(a,0)(\phi(0,b)-\phi(0,\beta))}\Big\}\frac{\partial S}{\partial\beta}d\beta, \end{aligned}$$

where $r_1 = R(0,0)$, $r_2 = S(0,0)$. Inspection of these equations reveals that (5.2) is satisfied if, either

$$\frac{\partial R}{\partial\alpha}\Big/r_1 = \frac{\partial S}{\partial\alpha}\Big/r_2, \qquad 0 \le \alpha \le a, \qquad \beta = 0, \tag{6.7}$$

$$\frac{\partial R}{\partial\beta}\Big/r_1 = \frac{\partial S}{\partial\beta}\Big/r_2, \qquad 0 \le \beta \le b, \qquad \alpha = 0, \tag{6.8}$$

or

$$\frac{\partial S}{\partial \alpha} = 0, \qquad \frac{\partial R}{\partial \alpha} = 0, \qquad 0 \leq \alpha \leq a, \qquad \beta = 0, \tag{6.9}$$

$$\frac{\partial S}{\partial \beta} = 0, \qquad \frac{\partial R}{\partial \beta} = 0, \qquad 0 \leq \beta \leq b, \qquad \alpha = 0. \tag{6.10}$$

From (6.7), on substituting for $\partial S/\partial \alpha$ from (4.6), we obtain

$$\frac{\partial R}{\partial \alpha} = -\left(\frac{r_1}{r_2}\right)\frac{\partial \phi}{\partial \alpha} R, \qquad \beta = 0, \tag{6.11}$$

while, on substituting for $\partial R/\partial \beta$ from (6.3) into (6.8), we get

$$\frac{\partial S}{\partial \beta} = \left(\frac{r_2}{r_1}\right)\frac{\partial \phi}{\partial \beta} S, \qquad \alpha = 0. \tag{6.12}$$

In the case of a plane net, equations (6.11), (6.12) describe logarithmic spirals, but in order to study the nets associated with (6.9), (6.10) we turn to the use of nodal coordinates.

7. Nodal coordinates

A three-dimensional extension of the system of nodal coordinates due to Mikhlin [3] is that in which the coordinates of a nodal point of three-dimensional net equal s, t and f measured, respectively, along the axes parallel to the α-, β- and n-lines. Now (cf. Fig. 2) we define unit vectors l, m and n in these respective directions at the nodal point so that the position vector of the node

$$\mathbf{r} = s\mathbf{l} + t\mathbf{m} + f\mathbf{n}; \tag{7.1}$$

on differentiating with respect to α, this equation leads, by (B.1), to

$$h_\alpha \mathbf{l} = s\frac{\partial \mathbf{l}}{\partial \alpha} + \frac{\partial s}{\partial \alpha}\mathbf{l} + t\frac{\partial \mathbf{m}}{\partial \alpha} + \frac{\partial t}{\partial \alpha}\mathbf{m} + f\frac{\partial \mathbf{n}}{\partial \alpha} + \frac{\partial f}{\partial \alpha}\mathbf{n}.$$

Taking the scalar product with m, by (B.3), we then get

$$s\frac{\partial \phi}{\partial \alpha} + \frac{\partial t}{\partial \alpha} = 0. \tag{7.2}$$

In the same way, differentiating (7.1) with respect to β and taking the scalar product with $\mathbf{l}$, we obtain, by (B.2) and (B.4),

$$-t\frac{\partial \phi}{\partial \beta} + \frac{\partial s}{\partial \beta} = 0. \tag{7.3}$$

By taking the scalar products of the α- and β-derivatives of (7.1) with n, on the other hand, we obtain a pair of equations governing the shape of the principal surface containing the net. Differentiating (7.1) with respect to n and taking scalar products with l and m we obtain, by (4.8),

$$\frac{\partial s}{\partial n} = 0, \tag{7.4}$$

$$\frac{\partial t}{\partial n} = 0, \tag{7.5}$$

and these equations reveal the fact that the n-lines are straight. Differentiating (7.2) with respect to β, we obtain, by (3.6) and (7.3)

$$\frac{\partial^2 t}{\partial\alpha\partial\beta} + \left(\frac{\partial\phi}{\partial\alpha}\frac{\partial\phi}{\partial\beta}\right) t = 0, \tag{7.6}$$

while on differentiating (7.3) with respect to α, we get by (3.6) and (7.2)

$$\frac{\partial^2 s}{\partial\alpha\partial\beta} + \left(\frac{\partial\phi}{\partial\alpha}\frac{\partial\phi}{\partial\beta}\right) s = 0. \tag{7.7}$$

By virtue of (3.6), Eqs. (7.6) and (7.7) are again instances of the telegraphy equations in which the two independent variables are the angle ϕ measured along the α- and β-curves. It is convenient, in view of this fact, to let α be equal to ϕ measured along α-lines, and to chose β equal to ϕ, measured along the β-lines. Then since $s(0,0) = 0$, $t(0,0) = 0$, we obtain from (7.6), (7.7) and (C.3)

$$t(a,b) = \int_{\substack{0\\ \beta=0}}^{a} J_0\left\{2\sqrt{(a-\alpha)b}\right\}\frac{\partial t}{\partial\alpha}d\alpha + \int_{\substack{0\\ \alpha=0}}^{b} J_0\left\{2\sqrt{a(b-\beta)}\right\}\frac{\partial t}{\partial\beta}d\beta, \tag{7.8}$$

$$s(a,b) = \int_{\substack{0\\ \beta=0}}^{a} J_0\left\{2\sqrt{(a-\alpha)b}\right\}\frac{\partial s}{\partial\alpha}d\alpha + \int_{\substack{0\\ \alpha=0}}^{b} J_0\left\{2\sqrt{a(b-\beta)}\right\}\frac{\partial s}{\partial\beta}d\beta. \tag{7.9}$$

In the case of a plane slip-line net (6.9), Eqs. (6.10) describe orthogonally intersecting circles and, if r_1, r_2 are the respective radii of these circles (describing α- and β-lines), the nodal coordinates on these circles are given by (see Fig. 3)

$$s = r_1 \sin\alpha + r_2(1 - \cos\beta),$$
$$t = r_2 \sin\beta + r_1(1 - \cos\alpha).$$

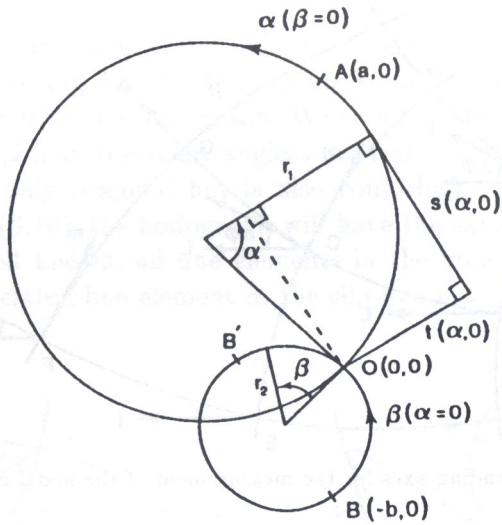

FIG. 3.

On substituting into (7.8), (7.9) we obtain

$$t = r_1 \int_0^a J_0\left\{2\sqrt{(a-\alpha)b}\right\} \sin\alpha \, d\alpha + r_2 \int_0^b J_0\left\{2\sqrt{a(b-\beta)}\right\} \cos\beta \, d\beta, \tag{7.10}$$

$$s = r_1 \int_0^a J_0\left\{2\sqrt{(a-\alpha)b}\right\} \cos\alpha \, d\alpha + r_2 \int_0^b J_0\left\{2\sqrt{a(b-\beta)}\right\} \sin\beta \, d\beta. \tag{7.11}$$

The axes **l** and **m**, along which these coordinates are to be measured are found as indicated in Fig. 4 [11]; the deviation $\Delta\phi$ equals the interval in ϕ between any two neighbouring nodes; the l-axes are parallel at the nodes A, C and F. For a net in which all the deviations between consecutive nodes are equal, this property extends to the family of nodal diagonals such as ACF, so that we need to determine only **l** and **m** at the nodal points on the boundary in order to determine these vectors at all the nodal points of the slip-line field.

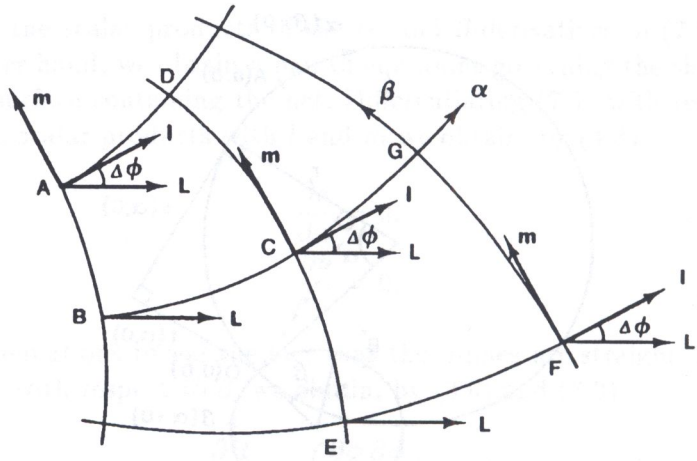

FIG. 4. Method of finding axes for the measurement of the nodal coordinates s and t.

8. THE VELOCITY HODOGRAPH

The velocity vector has only two components: u parallel to the α-lines and v parallel to the β-lines. Thus the velocity may be represented on a series of two-dimensional hodographs. By (D.2), (D.3) and (B.11), (B.12) we have

$$\frac{\partial u}{\partial \alpha} - v\frac{\partial \phi}{\partial \alpha} = 0, \tag{8.1}$$

$$\frac{\partial v}{\partial \beta} + u\frac{\partial \phi}{\partial \beta} = 0 \tag{8.2}$$

which, for plane slip-line fields, become GEIRINGERS equations [12]. If we differentiate (8.1) with respect to β and substitute from (8.2) and (3.6), we obtain

$$\frac{\partial^2 u}{\partial \alpha \partial \beta} + \left(\frac{\partial \phi}{\partial \alpha}\frac{\partial \phi}{\partial \beta}\right) u = 0, \tag{8.3}$$

while differentiating (8.2) and proceeding in a similar way we get

$$\frac{\partial^2 v}{\partial \alpha \partial \beta} + \left(\frac{\partial \phi}{\partial \alpha}\frac{\partial \phi}{\partial \beta}\right) v = 0. \tag{8.4}$$

Once again, due to (3.6), (8.3) and (8.4) are instances of the telegraphy equation. If we wish to use the hodograph, and OA, OB in the slip-line net of Fig. 5 a are boundary lines, then, since only the direction of the velocity vector can change along these lines, OA and OB give rise to the circular

arcs $O'A'$ and $O'B'$ in the velocity hodograph (Fig. 5 b). The vector shown by the solid arrow in Fig. 5 b has components u and v parallel, respectively, to the α- and β-lines in the hodograph. We should note in this connection that, since α and β may represent angles, the transformation from Fig. 5 a to Fig. 5 b is not only isogonal but is also conformal. It is clear that, in view of (6.9) and (6.10), the hodograph will have the same form as the net, although, as is well known, all line elements in the hodograph lie at right angles to the associated line element in the slip-line net.

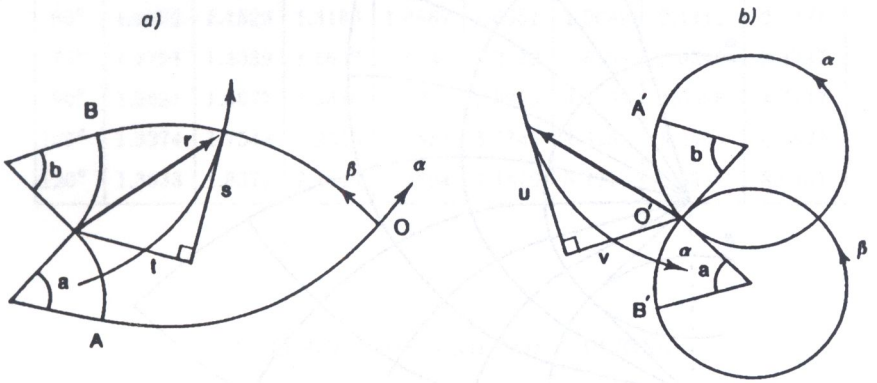

FIG. 5. Transformation from a slip-line net to its hodograph.

9. RESULTS

We define

$$F(a,b) = \int_0^a I_0\left\{2\sqrt{(a-\zeta)b}\right\} \sin\zeta\, d\zeta,$$

$$G(a,b) = \int_0^a I_0\left\{2\sqrt{(a-\zeta)b}\right\} \cos\zeta\, d\zeta,$$

where I_0 is the Bessel function of zero order and imaginary argument. Then (7.10), (7.11) become, for negative b (OB in Fig. 3),

$$t = r_1 F(a,b) + r_2 G(b,a), \tag{9.1}$$

$$s = r_1 G(a,b) + r_2 F(b,a), \tag{9.2}$$

while similar equations give u and v on the hodograph.

The integrals $F(a,b)$, $G(a,b)$ were computed numerically to within the accuracy of four decimal places, and the results of these computations are

given as entries in Tables 1 and 2. The net shown in Fig. 6 was constructed using these tables.

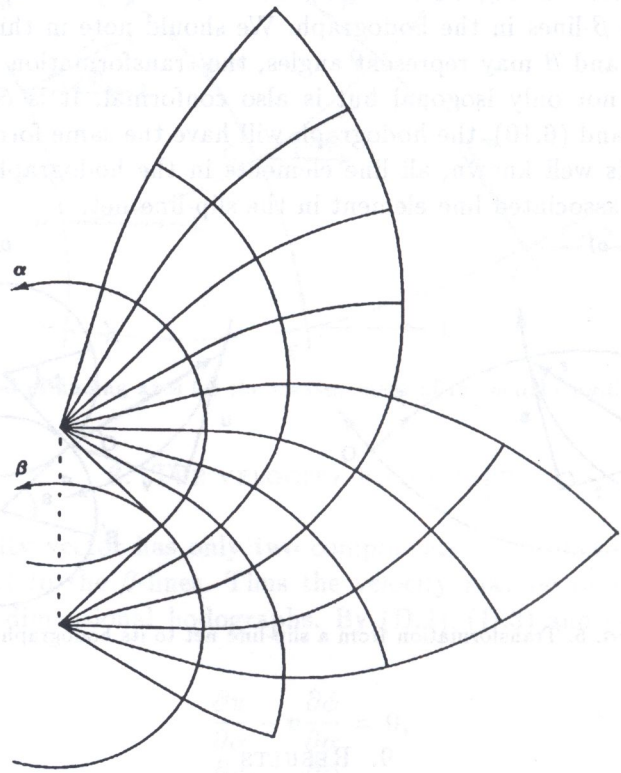

FIG. 6. Plane equi-angular net associated with a boundary consisting of two equal orthogonal circles.

Table 1. $F(a,b) = \int_0^a I_0\left\{2\sqrt{(a-\zeta)b}\right\} \sin\zeta\, d\zeta.$

a	$b = 15°$	$b = 30°$	$b = 45°$	$b = 60°$	$b = 75°$	$b = 90°$	$b = 105°$	$b = 120°$
15°	0.0348	0.0356	0.0364	0.0373	0.0381	0.0390	0.0398	0.0407
30°	0.1402	0.1467	0.1534	0.1603	0.1676	0.1753	0.1827	0.1907
45°	0.3139	0.3361	0.3593	0.3838	0.4096	0.4367	0.4651	0.4949
60°	0.5491	0.6017	0.6580	0.7182	0.7826	0.8512	0.9245	1.0026
75°	0.8350	0.9374	1.0488	1.1703	1.3016	1.4443	1.5989	1.7662
90°	1.1576	1.3328	1.5268	1.7413	1.9781	2.2389	2.5258	2.8407
105°	1.5013	1.7742	2.0828	2.4300	2.8195	3.2553	3.7420	4.2841
120°	1.8465	2.2458	2.7048	3.2302	3.8295	4.5108	5.2830	6.1560

Table 2. $G(a,b) = \int_0^a I_0\left\{2\sqrt{(a-\zeta)b}\right\}\cos\zeta\, d\zeta.$

a	$b = 15°$	$b = 30°$	$b = 45°$	$b = 60°$	$b = 75°$	$b = 90°$	$b = 105°$	$b = 120°$
15°	0.2678	0.2770	0.2865	0.2961	0.3060	0.3161	0.3264	0.3368
30°	0.5359	0.5734	0.6125	0.6536	0.6968	0.7427	0.7884	0.8373
45°	0.7865	0.8715	0.9626	1.0598	1.1637	1.2744	1.3924	1.5181
60°	1.0032	1.1529	1.3186	1.4987	1.6951	1.9089	2.1412	2.3934
75°	1.1721	1.4039	1.6637	1.9541	2.2772	2.6364	3.0345	3.4747
90°	1.2821	1.6077	1.9816	2.4089	2.8953	3.4467	4.0698	4.7717
105°	1.3274	1.7544	2.2585	2.8483	3.5345	4.3287	5.2435	6.2927
120°	1.3033	1.8374	2.4840	3.2594	4.1819	5.2717	6.5517	8.0467

10. Discussion and conclusions

The new principle leads to three-dimensional slip-line surfaces characterised by certain boundary configurations. In fact, in the case of a cold-worked metal the Hencky - Prandtl nets, if we may still so refer to these fields, are located on one of the three families of principal stress surfaces in the deforming solid. These surfaces may be curved or plane and the normal strain rates vanish. The slip-lines themselves are, in consequence, inextensible.

Equations (3.1) and (3.2) describe the deformation for which the distance between the n principal stress-surfaces remains constant, and Eqs. (7.4) and (7.5) confirm this fact by showing that the n-lines are straight. Moreover, from Eqs. (3.3) and (3.4) it follows that for an ideal solid, σ obeys the same equations as in the classical theory, provided that α and β are suitably re-defined.

Yet again in mechanics we encounter the Laplace equation in the form (4.9). Consistency with this new Eq. (3.6), which represents the requirements of stress equilibrium under the yield condition, demands that the ratio of the curvatures of the slip-lines, as measured in the tangent planes to the principal surfaces containing the net, must be constant. In the case of a plane net this condition requires that the boundary to the net should consist of either a pair of orthogonally intersecting logarithmic spirals, or of a pair of orthogonal circles. In the latter case the net has the form shown in

Fig. 6. The hodograph associated with this slip-line-field has the same form as the net; the fact is already known, although this is not the case when the boundaries are logarithmic spirals. The net shown in Fig. 6, when superposed over HILL'S equi-angular net [3], is found to match the latter precisely. HILL used his net to solve the plane strain compression problem [3] and he put forward a solution to this problem entirely different from that proposed by PRANDTL [2]. Prandtl's solution is not consistent with Eq. (5.2), and so it cannot describe the plane-strain compression of a cold-worked metal, while Hill's solution, on the other hand, does confirm to Eq. (5.2), and so it is consistent with the principle of continuity of the rotation rate. The material needs to be cold-worked for reasons that are outlined in Appendix E.

APPENDIX A. STRESS-EQUILIBRIUM

By considering the equilibrium of forces acting on the faces of a small prism, of side lengths $h_\alpha d\alpha$, $h_\beta d\beta$, $h_\gamma d\gamma$, and taking scalar products with the unit vectors **l**, **m** and **n** directed along the respective α, β and γ lines, we may obtain by means of (B.5)–(B.10) the three equations of stress-equilibrium, which also express the solenoidal property of the stress tensor. The l-, m- and n-equations, so obtained, are

$$\text{(A.1)}\quad \frac{\partial\sigma_{\alpha\alpha}}{h_\alpha\partial\alpha}+\frac{\partial\sigma_{\alpha\beta}}{h_\beta\partial\beta}+\frac{\partial\sigma_{\alpha\gamma}}{h_\gamma\partial\gamma}+\frac{(\sigma_{\alpha\alpha}-\sigma_{\beta\beta})}{h_\alpha h_\beta}\frac{\partial h_\beta}{\partial\alpha}+\frac{(\sigma_{\alpha\alpha}-\sigma_{\gamma\gamma})}{h_\alpha h_\gamma}\frac{\partial h_\gamma}{\partial\alpha}$$
$$+\frac{\sigma_{\alpha\beta}}{h_\beta}\left(\frac{2}{h_\alpha}\frac{\partial h_\alpha}{\partial\beta}+\frac{1}{h_\gamma}\frac{\partial h_\gamma}{\partial\beta}\right)+\frac{\sigma_{\alpha\gamma}}{h_\gamma}\left(\frac{2}{h_\alpha}\frac{\partial h_\alpha}{\partial\gamma}+\frac{1}{h_\beta}\frac{\partial h_\beta}{\partial\gamma}\right)=0,$$

$$\text{(A.2)}\quad \frac{\partial\sigma_{\beta\beta}}{h_\beta\partial\beta}+\frac{\partial\sigma_{\beta\gamma}}{h_\gamma\partial\gamma}+\frac{\partial\sigma_{\beta\alpha}}{h_\alpha\partial_\alpha}+\frac{(\sigma_{\beta\beta}-\sigma_{\gamma\gamma})}{h_\gamma h_\beta}\frac{\partial h_\gamma}{\partial\beta}+\frac{(\sigma_{\beta\beta}-\sigma_{\alpha\alpha})}{h_\alpha h_\beta}\frac{\partial h_\alpha}{\partial\beta}$$
$$+\frac{\sigma_{\beta\gamma}}{h_\gamma}\left(\frac{2}{h_\beta}\frac{\partial h_\beta}{\partial\gamma}+\frac{1}{h_\alpha}\frac{\partial h_\alpha}{\partial\gamma}\right)+\frac{\sigma_{\beta\alpha}}{h_\alpha}\left(\frac{2}{h_\beta}\frac{\partial h_\beta}{\partial\alpha}+\frac{1}{h_\gamma}\frac{\partial h_\gamma}{\partial\alpha}\right)=0,$$

$$\text{(A.3)}\quad \frac{\partial\sigma_{\gamma\gamma}}{h_\gamma\partial\gamma}+\frac{\partial\sigma_{\gamma\alpha}}{h_\alpha\partial\alpha}+\frac{\partial\sigma_{\gamma\beta}}{h_\beta\partial\beta}+\frac{(\sigma_{\gamma\gamma}-\sigma_{\alpha\alpha})}{h_\gamma h_\alpha}\frac{\partial h_\alpha}{\partial\gamma}+\frac{(\sigma_{\gamma\gamma}-\sigma_{\beta\beta})}{h_\gamma h_\beta}\frac{\partial h_\beta}{\partial\gamma}$$
$$+\frac{\sigma_{\gamma\alpha}}{h_\alpha}\left(\frac{2}{h_\gamma}\frac{\partial h_\gamma}{\partial\alpha}+\frac{1}{h_\beta}\frac{\partial h_\beta}{\partial\alpha}\right)+\frac{\sigma_{\gamma\beta}}{h_\beta}\left(\frac{2}{h_\gamma}\frac{\partial h_\gamma}{\partial\beta}+\frac{1}{h_\alpha}\frac{\partial h_\alpha}{\partial\beta}\right)=0.$$

Appendix B. Curvilinear coordinates

If α, β and γ are coordinates measured along orthogonal curves, then the scale factors, h_α, h_β and h_γ, for those respective curves, are defined so that $h_\alpha d\alpha$, $h_\beta d\beta$, and $h_\gamma d\gamma$ are length increments. Moreover, if $\mathbf{r}$ is the position vector of a point, then the unit vectors $\mathbf{l}$, $\mathbf{m}$ and $\mathbf{n}$, which lie parallel to the respective α-, β- and γ-curves, are given by

$$\mathbf{l} = \frac{\partial \mathbf{r}}{h_\alpha \partial \alpha}, \tag{B.1}$$

$$\mathbf{m} = \frac{\partial \mathbf{r}}{h_\beta \partial \beta}, \tag{B.2}$$

$$\mathbf{n} = \frac{\partial \mathbf{r}}{h_\gamma \partial \gamma}.$$

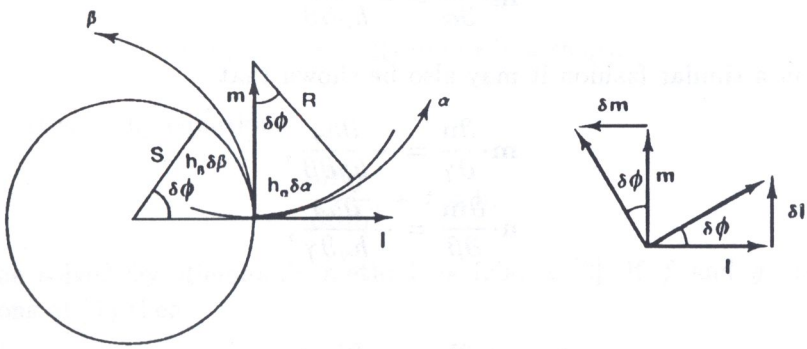

Fig. 7.

The vectors $\mathbf{l}$ and $\mathbf{m}$ and their increments are shown in Fig. 7, from which we see that for a small displacement along the α-lines

$$\mathbf{m} \cdot \delta \mathbf{l} = \delta\phi,$$

where ϕ is the net angle, or the rotation about $\mathbf{n}$. From this equation we obtain, on dividing by the associated increments in α and proceeding to the limit,

$$\mathbf{m} \cdot \frac{\partial \mathbf{l}}{\partial \alpha} = \frac{\partial \phi}{\partial \alpha}, \tag{B.3}$$

while in a similar fashion, we get for β-lines

$$\mathbf{l} \cdot \frac{\partial \mathbf{m}}{\partial \beta} = -\frac{\partial \phi}{\partial \beta}. \tag{B.4}$$

These equations serve to illustrate the sign convention that we use in connection with the slip-lines according to which the curvature of a slip-line is counted positive if its centre of curvature lies in the first quadrant of the plane tangent to the n-surface; otherwise the slip-line has negative curvature.

Applying the law of vector addition to the sides of a small loop in the n-surface with its sides parallel to the α- and β-lines, we may show that

$$\frac{\partial}{\partial\alpha}(h_\beta \mathbf{m}) = \frac{\partial}{\partial\beta}(h_\alpha \mathbf{l}),$$

and, on carrying out the dfferentiations and taking scalar products with $\mathbf{m}$ and $\mathbf{l}$, we obtain, respectively,

$$\mathbf{l}\cdot\frac{\partial \mathbf{m}}{\partial\beta} = -\frac{\partial h_\beta}{h_\alpha \partial\alpha}, \tag{B.5}$$

$$\mathbf{m}\cdot\frac{\partial \mathbf{l}}{\partial\alpha} = -\frac{\partial h_\alpha}{h_\beta \partial\beta}, \tag{B.6}$$

while in a similar fashion it may also be shown that

$$\mathbf{m}\cdot\frac{\partial \mathbf{n}}{\partial\gamma} = -\frac{\partial h_\gamma}{h_\beta \partial\beta}, \tag{B.7}$$

$$\mathbf{n}\cdot\frac{\partial \mathbf{m}}{\partial\beta} = -\frac{\partial h_\beta}{h_\gamma \partial\gamma}, \tag{B.8}$$

and

$$\mathbf{n}\cdot\frac{\partial \mathbf{l}}{\partial\alpha} = -\frac{\partial h_\alpha}{h_\gamma \partial\gamma}, \tag{B.9}$$

$$\mathbf{l}\cdot\frac{\partial \mathbf{n}}{\partial\gamma} = -\frac{\partial h_\gamma}{h_\alpha \partial\alpha}. \tag{B.10}$$

From (B.3), (B.4), (B.5) and (B.6) we obtain

$$\frac{\partial h_\alpha}{\partial\beta} = -h_\beta \frac{\partial\phi}{\partial\alpha}, \tag{B.11}$$

$$\frac{\partial h_\beta}{\partial\alpha} = h_\alpha \frac{\partial\phi}{\partial\beta}. \tag{B.12}$$

The scale factors may be related to the radii of curvature as follows. Letting R denote the radius of curvature of the α-lines in the plane tangent to the n-surface, it is clear from Fig. 7 that

$$R\delta\phi = h_\alpha \delta\alpha,$$

or

$$R\frac{\partial\phi}{\partial\alpha} = h_\alpha . \tag{B.13}$$

In the same way, if S denotes the radius of curvature of the β-lines, we may show that

$$S\frac{\partial\phi}{\partial\beta} = -h_\beta . \tag{B.14}$$

We require, in addition to the above formulae, the equation for the Laplacian. This is obtained by evaluating the divergence of a gradient. Thus we obtain

$$h_\alpha h_\beta h_\gamma \nabla^2 = \frac{\partial}{\partial\alpha}\left(\frac{h_\beta h_\gamma}{h_\alpha}\frac{\partial}{\partial\alpha}\right) + \frac{\partial}{\partial\beta}\left(\frac{h_\gamma h_\alpha}{h_\beta}\frac{\partial}{\partial\beta}\right) + \frac{\partial}{\partial\gamma}\left(\frac{h_\alpha h_\beta}{h_\gamma}\frac{\partial}{\partial\gamma}\right). \tag{B.15}$$

Appendix C. Riemann's method

The telegraphy equation,

$$\frac{\partial^2 f}{\partial\alpha\partial\beta} + f = 0, \tag{C.1}$$

may be solved by Riemann's method as follows [2]. If f and g are two solutions of (1) then

$$\left(g\frac{\partial f}{\partial\alpha} - f\frac{\partial g}{\partial\alpha}\right)d\alpha - \left(g\frac{\partial f}{\partial\beta} - f\frac{\partial g}{\partial\beta}\right)d\beta$$

will be a total differential as the reader may readily verify. On integrating this expression around a contour made up of α- and β-lines, such that $\alpha = 0$, $0 \leq \beta \leq b$ and $\beta = 0$, $0 \leq \alpha \leq 2$ are boundary lines, we obtain

$$\int_0^a \left(g\frac{\partial f}{\partial\alpha} - f\frac{\partial g}{\partial\alpha}\right)d\alpha - \int_0^b \left(g\frac{\partial f}{\partial\beta} - f\frac{\partial g}{\partial\beta}\right)d\beta + \int_a^0 \left(g\frac{\partial f}{\partial\alpha} - f\frac{\partial g}{\partial\alpha}\right)d\alpha - \int_b^0 \left(g\frac{\partial f}{\partial\beta} - f\frac{\partial g}{\partial\beta}\right)d\beta = 0. \tag{C.2}$$

Moreover, we may choose for g the function

$$g = J_0\left\{2\sqrt{(a-\alpha)(b-\beta)}\right\},$$

where $J_0(t)$ is the Bessel function of the first kind and zero order because this function satisfies the equation obtainable from (C.1):

$$J_0''(t) + \frac{1}{t}J_0'(t) + J_0(t) = 0.$$

We then have

$$\begin{aligned} g &= 1 \quad \text{for} \quad \alpha = a, \\ g &= 1 \quad \text{for} \quad \beta = b, \\ \frac{\partial g}{\partial \alpha} &= 0 \quad \text{for} \quad \beta = b, \\ \frac{\partial g}{\partial \beta} &= 0 \quad \text{for} \quad \alpha = a, \end{aligned}$$

while in (C.2) we may integrate

$$\int_0^a f\frac{\partial g}{\partial \alpha}d\alpha \quad \text{and} \quad \int_0^b f\frac{\partial g}{\partial \beta}d\beta$$

by parts, obtaining

$$\text{(C.3)} \qquad f(a,b) = J_0\left\{2\sqrt{ab}\right\}f(0,0) + \int_0^a J_0\left\{2\sqrt{(a-\alpha)b}\right\}\frac{\partial f}{\partial \alpha}d\alpha + \int_0^b J_0\left\{2\sqrt{a(b-\beta)}\right\}\frac{\partial f}{\partial \beta}d\beta.$$

This equation provides the value of f at the point (a,b) of the net in terms of the boundary values of the derivatives of f along the boundary lines $\alpha = 0$, $0 \leq \beta \leq b$ and $\beta = 0$, $0 \leq \alpha \leq a$.

Appendix D. Strain rates

If $\mathbf{v}$ denotes the velocity vector associated with a point in a deforming body and $d\mathbf{e}$ is the vector representing the extension rate of the straight line connecting two neighbouring points in the body, while the rigid body rotation rate, $\boldsymbol{\omega}$, is defined by

$$\boldsymbol{\omega} = (1/2)\,\mathrm{curl}\,\mathbf{v},$$

then the difference of the vector velocities of two neighbouring points of the body is equal to

$$\text{(D.1)} \qquad d\mathbf{v} = d\mathbf{e} + \boldsymbol{\omega} \times d\mathbf{r}.$$

Thus, noting that $\dot{\varepsilon}_{\alpha\alpha}$ is the coefficient of $h_\alpha d\alpha$ in $\mathbf{l}\,de$ and $\dot{\varepsilon}_{\beta\beta}$ of $h_\beta d\beta$ in $\mathbf{m}\,de$, we obtain, on taking the scalar products of (D.1) with $\mathbf{l}$ and $\mathbf{m}$ and using (B.5), (B.6), (B.8) and (B.9), the equations

$$\dot{\varepsilon}_{\alpha\alpha} = \frac{\partial v_\alpha}{h_\alpha \partial\alpha} + \frac{v_\beta}{h_\alpha h_\beta}\frac{\partial h_\alpha}{\partial\beta} + \frac{v_\gamma}{h_\alpha h_\gamma}\frac{\partial h_\alpha}{\partial\gamma}, \tag{D.2}$$

$$\dot{\varepsilon}_{\beta\beta} = \frac{\partial v_\beta}{h_\beta \partial\beta} + \frac{v_\gamma}{h_\gamma h_\beta}\frac{\partial h_\beta}{\partial\gamma} + \frac{v_\alpha}{h_\alpha h_\beta}\frac{\partial h_\beta}{\partial\alpha}. \tag{D.3}$$

Appendix E

As a metallic body is cold-worked, its crystal grains begin to rotate so as to align their planes of crystallographic slip parallel to the principal shear surfaces within that body. Of course, the crystal grains cannot rotate rigidly, but they turn by means of double- (or multiple-) slip, on two (or more) intersecting planes of crystallographic shear. Each crystal-grain rotates as an assemblage of small sliding (or "slipping") rigid (more accurately elastic) bodies. During deformation the crystal grains, by this process, continue to maintain a state of alignment in which each active crystallographic slip-plane within a crystal-grain remains instantaneously parallel to a surface of principle shear. That is why the rotation rate remains spatially continuous in a heavily cold-worked metal undergoing plastic deformation; however, this principle cannot be applied to an annealed metal in which the crystal-grains are not mutually aligned.

Simple expriments have been described in [10] by means of which the hypothesis of continuity of the rotation rate may be tested, although the very first observations on the subject of crystallographic alignments in cold-worked metals were made early in this century, the experiments described by Rosenhain [13] being particularly noteworthy. More recently, the spectacular photomacrographs obtained by French and Weinrich [14], showing cascades of shear-lines in the necked regions of slowly deforming tensile test samples, testify to the truth of the assertions on which the principle of continuity of the rotation rate rests.

References

1. R.L. Bish, *Plane-stress deformation of a flat plate by slip between elastic elements*, Arch. Mech., **46**, 3–12, 1994.

2. L. PRANDTL, *Über die Harte plastischer Körper*, Nachrichten von der Königlichen Gesellschaft der Wissenschafen zu Götingen, Mathematisch-Physikalische Klasse, **13**, 74–85, 1920.

3. R. HILL, *The mathematical theory of plasticity*, Oxford University Press, 1950.

4. A. NADAI, *Plasticity*, McGraw-Hill, 1931.

5. W. PRAGER and P.G. HODGE, *Theory of perfectly plastic solids*, Chapman and Hall Ltd., 1951.

6. W. JOHNSON and P.B. MELLOR, *Plasticity for mechanical engineers*, D. van Nostrand Co. Ltd., 1962.

7. W. PRAGER, *Recent developments in plasticity*, J. Appl. Phys., **20**, 235–241, 1949.

8. W.T. KOITER, *Stress-strain relations, uniqueness and variational theorems for elastic-plastic materials with a singular yield surface*, Quart. Appl. Math., **11**, 350–354, 1953.

9. P. PERZYNA, *The constitutive equations for rate-sensitive plastic materials*, Quart. Appl. Math., **20**, 321–332, 1963.

10. R.L. BISH, *Transverse deflection of a cold-worked metal plate clamped around its edge*, Arch. Mech., [accepted for publication].

11. R. VON MISES, *Bemerkungen zur Formulierung des mathematischen Problems der Plastizitätstheorie*, Zeits. für Angew. Math. und Mech., **5**, 147–149, 1925.

12. H. GEIRINGER, *Beitrag zum vollständigen ebenen Plastizitätsproblem*, Int. Congr. Appl. Mech., 3rd proceedings, Comptes Rendus. Verhandlungen. Stockholm, **2**, 185–190, 1930.

13. W. ROSEHAIN, *An introduction to the study of physical metallurgy*, Constable and Co. Ltd., London 1915.

14. L.E. FRENCH and P.F. WEINRICH, *The tensile fracture mechanisms of fcc metals and alloys – a review of the influence of pressure*, J. Aust. Inst. Metals, **22**, 40–50, 1977.

AERONAUTICAL AND MARITIME RESEARCH LABORATORY, MELBOURNE, AUSTRALIA.

Received November 23, 1995.